INTERNATIONAL JOURNAL OF INTEGRATED ENGINEERING
ISSN: 2229-838X e-ISSN: 2600-7916

IJIE

Vol. 16 No. 3 (2024) 358-375
https://publisher.uthm.edu.my/ojs/index.php/ijie

Mathematical Modeling and Optimization of Process Parameters in 3D Printing of AlFeSi10Mg Components Using Neural Network and RSM

Kalluru Madhurima[1]*, Dr.K.Devaki Devi[2]

[1] *JNTUA, Mechanical Department,*
GPREC Research Centre, Kurnool, AP, INDIA
[2] *Mechanical Department,*
G Pulla Reddy Engineering College, Kurnool, AP, INDIA

*Corresponding Author: madhurima5012@gmail.com
DOI: https://doi.org/10.30880/ijie.2024.16.03.031

Article Info

Received: 18 March 2024
Accepted: 7 October 2024
Available online: 24 November 2024

Keywords

Additive manufacturing, SLM, AlSi10Mg, optimization

Abstract

Selected laser melting (SLM) products made of aluminum have been widely employed in biomedical, industries, and aerospace. However, SLM's unique process parameters make it difficult to efficiently print desired objects. SLM can be used to print high-strength aluminum alloys that can be optimized for processing. For parameter optimization of Scanning Speed, hatching distance, Layer height, and laser speed, the D-optimal design of experiments approach is utilized. We develop parameter windows for these three parameters (LED, SED, VED) about part density using 36 samples. The density data collected from the samples via analysis software agrees well with the numerical model calculated. SLM printing of Al products requires a pre-processing optimization system because SLM demands so much time, money, and professional understanding of the process and materials. An SLM optimization system based on a supervised artificial neural network is created in this research. The ideal SLM process parameters, which may be employed to manufacture a product that meets a user's need, are the outputs of this optimization method. An SLM operator does not require a lot of knowledge or a lot of time to experiment with this optimization system to print a suitable result. This system is a very important element in the pre-processing of SLM printing.

1. Introduction

In many industries, large numbers of identical parts are produced to reduce production costs. Due to the lower manufacturing costs per part, the higher piece count per batch corresponds to the production process concentrating on one type of component. Because of this, all the parts could be produced at a low cost, but a second piece would be extremely difficult or even impossible [1]-[3].

Because of this, designers had to create a single piece to fulfill it serves purpose, but it must also be able to be made according to the manufacturing process, which is also termed "design to manufacture". As a result, the manufacturing process severely restricts the part's complexity. Increasingly complex components have necessitated the development of new manufacturing processes that can produce them.[4]. The applications of additive manufacturing (AM) in such cases, where conventional manufacturing is ineffective, are excellent. As an alternative to using traditional manufacturing processes, rapid prototyping, also known as 3D printing, can be used to produce parts conventional manufacturing techniques, such as computer numerical control (CNC),

subtract material from main pieces to achieve desired geometries, while additive manufacturing adds material to the main part to achieve the desired geometry [5]-[10].

What is the market impact of all these different methods after being exposed to the major technologies? AM alters the manufacturing guidelines [7]. The following are some of its most important benefits:

1. Tooling: In traditional manufacturing, each piece requires a large number of tools and specialized equipment. There are no such restrictions when employing 3D printing; Only a machine and the material to be printed on are required.
2. Time to market: When compared to other manufacturing techniques, additive manufacturing (AM) is fast. Traditional manufacturing necessitates the purchase of equipment and tooling before the major production process can begin. When the machine is available, the procedure can start as early as the document is prepared, and the part will be completed very quickly. Being slightly quicker allows a manufacturing organization to detect problems, malfunctions, and mistakes more quickly, saving time and money[8].
3. Creativity: Although this new manufacturing technique allows for a wider choice of geometries, designers can let their imaginations run free while focusing on the part's purpose, sometimes known as "design to performance." Figure 1 illustrates several 3D-printed complicated pieces with a variety of geometries.
4. Customization: As previously stated, traditional techniques are typically focused on a single design, with the majority of pieces sharing a common geometry. Even minor alterations in the parts could result in significant costs for the organization[9]. Parts can be personalized and customized at will with 3D printing [11].
5. Material reduction: when the most complicated geometries can be created, a part that is more concentrated on its function can be created. This leads to waste reduction and, as a result, a reduction in costs.
6. No need for spare parts: Businesses require a huge inventory of spare parts to replace them if they break or malfunction. If a component is damaged or broken when using the AM system, it can be quickly replaced using simply the necessary part file[12].

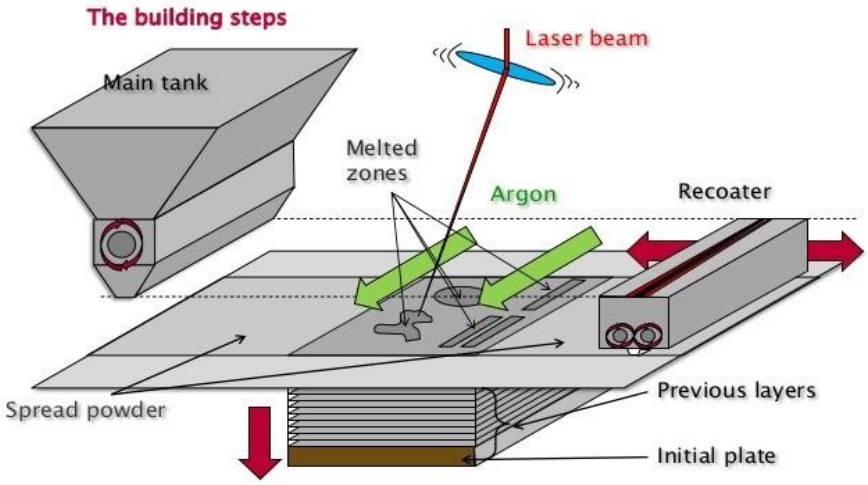

Fig. 1 *Schematic diagram for selective laser melting*

Among them are difficulty, small production sizes, and lower production time. All of these capabilities apply to a variety of industries, including medical, aerospace, robotics, and prototype, which is why these industries are the primary clients of AM and 3D printing. Even though certain processes are more appropriate than others, the client must choose which one to utilize in each case [13]-[16].

2. Selective Laser Melting (SLM)

2.1 Processing

Once the machine as well as the SLM setup, there are several tasks to complete, like constructing the data source that the machine is using for the manufacturing operation (SLM file)[16]. STL is now the most popular system for all 3D printing techniques. The specific part is defined by a collection of geometric shapes that describe the models' limits; there is no color, Surface roughness, or other type of feature in the documents. The number of

Int. Journal of Integrated Engineering Vol. 16 No. 3 (2024) p. 358-375

triangles used to designate a part, the higher the resolution, but the more difficult it is to function with this document. As a result, the fewer triangles in the SLM file, the better, but it should always include enough to ensure the part's pixel density and effectiveness of the part. The very same part from left to right, but with very few triangles and so less response. Using the STL document, the technology can be used to divide this design into 2D layers ranging in height from 20 to 100 μm. When the file is finished, each of these slices will be one of the build task's layers. The slicing procedure and choosing the parameters set can be done using a variety of tools; however, a Design Expert was utilized in this case. While the computer is creating the slices, it must select all the building characteristics that will be employed, such as distance, power, and so on[17].

2.2 Parameters

2.2.1 Layer Height (h)

As previously stated, additive manufacturing creates 3D parts by layering 2D slices, therefore the distance between each layer must be chosen at some point throughout the procedure. The distance between the layers, also known as layer thickness or layer height, should be between 0.02mm and 0.1mm. Because fewer layers are necessary to obtain the same length, the larger the above value, the faster the task will be. It is also visible in the build rate coefficient, which can be used to differentiate process productivity. The volume of material generated every 60 minutes is represented by this parameter, which is commonly given in cm^3/h. The product of scanning speed(V), layer height(H), and hatching distance(t) gives this equation.

$$B = h * t * v \tag{1}$$

As previously said, the build rate is directly proportional to layer height, thus the higher the value, the more productive the process will be. Because the time of the number of treatment options is not taken into account, the number of layers has a larger impact on the processing time, even if it is not represented in the build rate [18]. The platform is filled in 5 to 8 seconds by the recoater. When the layers are repeated by these few seconds, which is usually greater than 2.000, the recoating duration can easily exceed 2 hours.

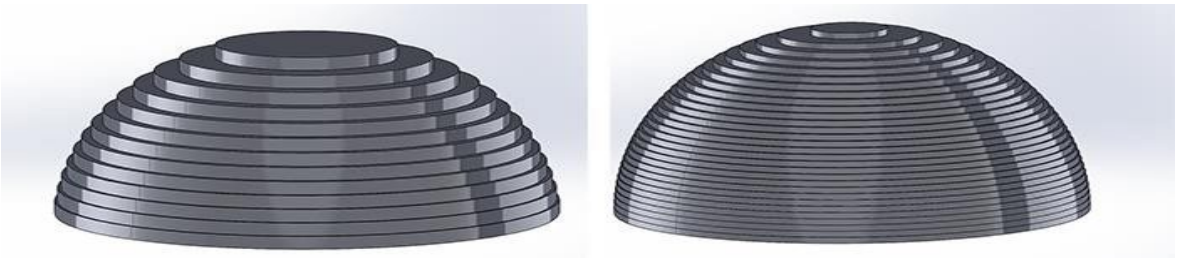

Fig. 2 *Resolution of the layers*

Fig. 2 The left part has a higher layer height and it will print rapidly due to fewer layers to produce, but the right part has a better resolution. The greater this value, on the other hand, the poorer the part's resolution. The effect of layer height on the part's resolution. Furthermore, if the space is too large, it might lead to poor layer attachment and part failure. For all of this, the layer height must be as high as feasible while remaining short enough to maintain layer adhesion and avoid any breakdowns.

2.2.2 Hatching Distance (t)

As illustrated in the slice view in Figure 3, the laser beam cuts a straight track over the target area to melt the powder. Hatching distance, also known as track distance, is the distance between two adjacent laser beam tracks. This measurement is in millimeters and can be anywhere from 0.05 and 0.25 millimeters. Whenever the laser beam reaches the powder bed, it sucks up the energy and melts a limited area. The diameter of the beam determines the surface of this region, which can be idealized as a circle [19].

It's essential to know that the distance between hatching refers to the distance between consecutive laser beam lines in the middle of the centers. The faster the build rate and production, the higher the layer height and hatching distance. If the tracks are too wide apart, as seen in Figure 2, the powder between them will not melt correctly. Furthermore, when a laser beam melts a circle, the energy in the outer zone is typically smaller than in the core. This indicates that certain zones have not melted properly, necessitating closer track spacing. Some powder is stroked by two different laser directions as a result of the tracks switching.

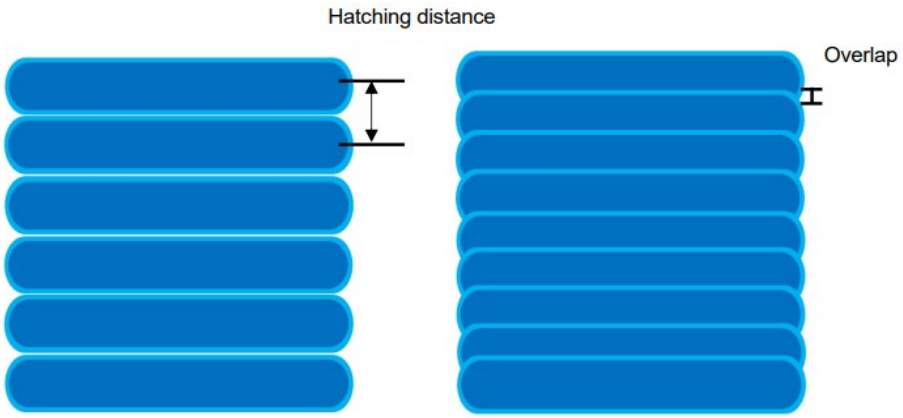

Fig. 3 *Hatching distance, like build rate, has a significant impact on part quality*

2.2.3 Laser Power (P)

The main energy source for powder melting is the laser beam's power, denoted in W. The higher the value, the more energy is transferred to the powder, which results in a high temperature. To meet all of the powder; more power may be required depending on the material to be printed. If the power is insufficient, the powder will not melt properly, causing the component to have porosity and a lower relative density. On the other side, if there is too much force, the powder will evaporate, resulting in flaws. Typically, SLM machines are equipped with lasers with a maximum power of 200-1.000W.

As previously stated, the scanning speed value must be determined to choose the appropriate power value. The speed directly affects the time spent in the same location, while the power represents the quantity of energy transferred every second. As a result, both numbers will determine how much energy is transported in this location. Furthermore, as previously said, the energy must be properly chosen; too much or too little energy will result in the creation of pores [20].

2.2.4 Scanning Speed (V)

Scanning speed is the velocity of the laser beam, measured in millimeters per second. The build rate is calculated by dividing its value by the hatching distance and layer height. The laser beam's speed should be adjusted to get the best possible production, but keep in mind that if it's too fast, it'll spend less time in the same location. The powder bed will receive less energy from the transfer, which will reduce the melting power and cause imperfections like pores to appear. As a result, if the scanning speed is very slow, the laser can end up evaporating powder and causing pores as well [21]. For this reason, it is important to choose the scanning speed carefully. There is a very close relationship between speed and power, and oftentimes, modifications made to either of them cause changes in the other. The speed range, for example, can be varied by the power utilized, the material being printed, and so on; it can range from 300 to 2.500 mm/s.

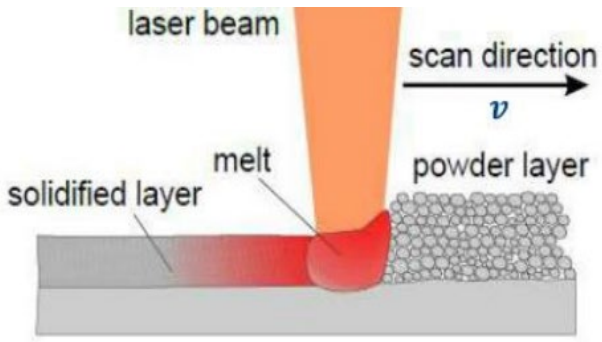

Fig. 4 *The SLM process is depicted in this diagram, which shows how the laser melts the powder bed*

Int. Journal of Integrated Engineering Vol. 16 No. 3 (2024) p. 358-375

2.2.5 LED, SED, and VED

The above-mentioned parameters are those that are set during the build job generation process, and their values are inserted into the program's parameters set. Other significant parameters to consider that cannot be altered when programming the build job are as follows. Those parameters can be calculated using the previous ones. As a result, they should be calculated before the other factors stated previously. These parameters are presented in the following manner, with a diagram in Figure 4 to help understanding:

1. The linear energy density refers to the quantity of energy given to the powder bed in a straight line (LED). When you divide the scanning speed by the power, you get this. The outcome's unit of measurement is J/mm.
2. SED (Surface Energy Density) is expressed in J/mm^2 and is determined by dividing the LED by the hatching distance. It is the energy delivered to the stroked surface by the laser beam.
3. The amount of energy delivered by the laser beam to the working volume is measured in Volume Energy Density (VED). It is calculated in J/mm^3 and is determined by dividing the surface energy density by the layer height[22].

$$B=h*t*v \tag{1}$$

$$\mathrm{LED} = \mathrm{P/V} \tag{2}$$

$$\mathrm{SED} = \mathrm{P/V} * \mathrm{H} \tag{3}$$

$$\mathrm{VED} = \mathrm{P/V} * \mathrm{H} * \mathrm{T} \tag{4}$$

3. The Material: AlFeSi10Mg

With its excellent characteristics and processing capabilities, aluminum is one of the most widely utilized metals on the planet. It's a light metal with a density of 2.67g/cm^3, which, combined with its high strength, makes it ideal for applications where the load of the part is critical. When it comes to the SLM technique, AlFeSi10Mg is the most popular aluminum alloy [23]. Its features make it an excellent choice for creating complicated geometries with thin walls, which are ideal for SLM processing. As a result, this material is widely used in SLM procedures in industries such as automotive, aerospace, and prototypes. SLM Solutions delivered the powder, which came from the same batch and came with a certificate detailing all of its features. This document covers all the powder's data, including particle size, chemical composition, and shape, among other things.

The chemical composition of AlFeSi10Mg is represented in where approximately 9-11% of Si content and 0.2-0.45% of Mg content is present in the alloy, together with small portions of Cu, Zn, and Fe content. The maximum useful limit of Mg content in the alloy is approximately 0.7 wt%. The powder has an obvious density of 1.25g/cm^{3}Due to the amount of air between the particles, aluminum has a density of 2.67g/cm^3.

4. Design of Experiments (DOE)

The Experimental design is the analysis of the most essential factors impacting characteristics, as well as a schedule for carrying out such experimentations.

4.1 Response Surface Methodology (RSM)

The RSM is a numerical method for making a numerical model for analysis and optimization [24]. The Input machining parameters can be used to show the output responses such as LED, SED, and VED using experiment trials and regression analysis[25]-[29]. The major steps in response surface methodology:

1. Determination of the most important elements, such as hatching distance, laser speed, laser power, and layer height.
2. Creating an experimental design matrix and performing the experiments according to the design matrix.
3. Constructing a numerical methods model.
4. Calculation of the created model's constant coefficients.
5. The significance of the coefficients is tested.
6. Using analysis of variance do an adequacy test on the created model (ANOVA).
7. Examining the impact of input machining parameters on output outcomes.

Table 4.1 *Experimental observations*

Run	Factor1	Factor2	Factor3	Factor4	Response1	Response2	Response3
	P: Power	V: Speed	H: Layer Height	T: Layer Thickness	R1: LED	R2: SED	R3: VED
	w	mm/sec	mm	mm	j/mm	j/mm2	j/mm3
1	325	1100	0.25	0.03	0.295	14.777	39.39
2	295	1300	0.125	0.06	0.226	3.8	30.05
3	317	1000	0.25	0.04	0.317	7.93	32.01
4	370	900	0.173	0.04	0.411	10.28	79.05
5	370	1300	0.25	0.02	0.284	14.23	57.22
6	370	955	0.15	0.02	0.387	19.37	129.45
7	370	1270	0.15	0.05	0.291	5.83	31
8	314	900	0.199	0.06	0.348	5.81	30.89
9	295	1100	0.125	0.03	0.268	8.94	71.55
10	310	1270	0.25	0.05	0.244	4.88	16.7
11	325	1250	0.25	0.04	0.26	6.5	25.745
12	325	1300	0.15	0.03	0.25	8.33	56.05
13	370	1235	0.1	0.04	0.3	7.49	74.68
14	370	1300	0.25	0.02	0.284	14.2	56.02
15	370	1270	0.15	0.03	0.291	7.3	49.61

4.1.1 Response 1

Table 4.2 *Fit summary R1 LED*

Source	Adjusted R^2	Predicted R^2	Sequential p-value	Lack of Fit P-value	
Linear	0.4317	0.3744	< 0.0001		
2FI	0.6914	0.6170	< 0.0001		
Quadratic	0.7438	0.6732	0.0025		Suggested
Cubic	0.8517	0.7338	< 0.0001		Aliased

Table 4.3 *ANOVA for the response surface quadratic model of LED*

Source	Sum of Squares	of	Mean Square	F-value	p-value
Model	0.5663	10	0.056	26300	<.0001
A-power	0.0015	1	0.001	689.1	<.0001
B-Speed	0.0003	1	0.000	125.7	< 0.0001
C-Hatching Distance	0.0000	1	0.000	10.7	0.0054
D-Layer thickness	2.536E-06	1	2.536E-0	1.1	0.2961
AB	0.0005	1	0.0005	233.8	< 0.001
AC	0.0000	1	0.00	16.5	0.0011
AD	2.154E-06	1	2.154E-06	1	0.3342

Int. Journal of Integrated Engineering Vol. 16 No. 3 (2024) p. 358-375

BC	1.112E-06	1	1.112E-06	0.51	0.4841
BD	6.773E-06	1	6.773E-06	3.15	0.0979
CD	0.0000	1	0.00	9.65	0.0077
Residual	0.0000	14	2.153E-06		
Lack of Fit	0.0000	4	7.536E-06		
Pure Error	0.0000	10	0.00		
Cor Total	0.5663	24			

Based on Table 4.3 the experiment's findings used the dependable statistical method of ANOVA to investigate the impact of process elements. Components A, B, C, AB, AC, and CD had significant p-values (0.0500) indicating their influence. The strong model was demonstrated by the high F-value (26300.17). Close R^2 values showed the ability to forecast (predicted: 0.9990, adjusted: 0.9999). Adeq Precision Ratio (420.915) was higher than the cutoff of 4, highlighting dependability. Complex associations were deciphered by ANOVA, giving insights from complex data.

4.1.2 Response 2

Table 4.4 *Fit summary SED*

Source	Adjusted R^2	Predicted R^2	Sequential p-value	Lack of Fit P-value	
Linear	0.3903	0.3398	< 0.0001		
2FI	0.4875	0.3978	0.0053		
Quadratic	0.6993	0.6189	< 0.0001		Suggested
Cubic	0.9250	0.8607	< 0.0001		Aliased

4.1.3 Response 2: SED

Table 4.5 *ANOVA for the response surface quadratic model of SED*

Source	Sum of Squares	of	Mean Square	F-value	p-value	
Model	781.59	11	71.05	821.85	0.0001	Significant
A-power	0.9130	1	0.9130	10.56	0.006	
B-Speed	1.94	1	1.94	22.46	0.0004	
C-Hatching Distance	13.27	1	13.27	153.5	0.000	
D-Layer thickness	0.9344	1	0.9344	10.81	0.005	
AB	7.47	1	7.47	86.40	0.0001	
AC	15.96	1	15.96	184.5	0.0001	
AD	8.98	1	8.98	103.8	0.0001	
BC	0.4116	1	0.4116	4.76	0.0481	
CD	9.47	1	9.47	109.5	0.0001	
A^2	3.11	1	3.11	36.01	0.0001	
D^2	20.71	1	20.71	239.5	0.0001	
Residual	1.12	13	0.0865			
Lack of fit	0.2235	3	0.0745	0.827	0.5084	

Pure Error	0.9005	10	0.0900			
Cor Total	782.72	24				
Model	781.59	11	71.05	821.85	0.0001	Significant

The data is the result of a careful investigation of a statistical model that was probably created using regression analysis or experimental DoE. Model relevance is confirmed by a significant F-value of (821.85); specific models (A, B, C, D, AB, AC, AD, BC, CD, A^2, D^2) are supported by p-values of less than 0.0500. Small discrepancies are implied by an F-value of 0.83 which indicates a modest lack of fit. Model robustness is indicated by constant anticipated R^2 (0.9921) and adjusted R^2 (0.9973) values as shown in Table 4.5. Key data patterns are highlighted by a strong signal ratio (95.086). The model successfully captures changeable relationships, enabling comprehension and improvement.

4.1.4 Response 3

Table 4.6 *Fit summary VED*

Source	Adjusted R^2	Predicted R^2	Sequential p-value	Lack of Fit P-value	
Linear	0.3144	0.2526	< 0.0001		
2FI	0.4715	0.3588	0.0004		
Quadratic	0.5906	0.4716	0.0003		Suggested
Cubic	0.8116	0.6388	< 0.0001		Aliased

4.1.5 Response 3: VED

Table 4.7 *ANOVA for the VED response surface quadratic model of VED*

Source	Sum of Squares	of	Mean Square	F-value	p-value	
Model	27753.21	13	2134.86	19365.6	<0.0001	Significant
A-power	37.03	1	37.03	335.9	0.0001	
B-Speed	219.58	1	219.58	1991	0.0001	
C-Hatching Distance	93.01	1	93.01	843.7	0.0001	
D-Layer thickness	0.1320	1	0.1320	1.20	0.2973	
AB	39.80	1	39.80	361.0	0.0001	
AC	35.74	1	35.74	324.2	0.0001	
AD	28.38	1	28.38	257.4	0.0001	
BD	25.37	1	25.37	230.1	0.0001	
CD	156.61	1	156.61	1420	0.0001	
A^2	35.47	1	35.47	321.7	0.0001	
B^2	63.59	1	63.59	576.8	0.0001	
C^2	383.89	1	383.89	3482.	0.0001	
D^2	150.77	1	150.77	1367.	0.0001	
Residual	1.21	11	0.1102			
Lack of fit	0.4926	1	0.4926	6.84	0.0258	Significant
Pure Error	0.7200	10	0.0720			

The model's outcomes are significant, as shown by Table 4.7, and a strong F-value of 19365.60 suggests that they are likely significant. It should be noted that terms A, B, C, AB, AC, AD, BD, CD, A^2, B^2, C, and D are deemed significant if their Pearson correlation coefficients are lower than 0.0500. With the lowest residual error and fitting adequacy indicated by the lack of fit F-value of 0.258, the model also demonstrates a solid fit. The expected R^2 of 0.9154 is very similar to the corrected R^2 of 0.9999. The ratio of 520.778 indicates the presence of a strong signal.

Int. Journal of Integrated Engineering Vol. 16 No. 3 (2024) p. 358-375

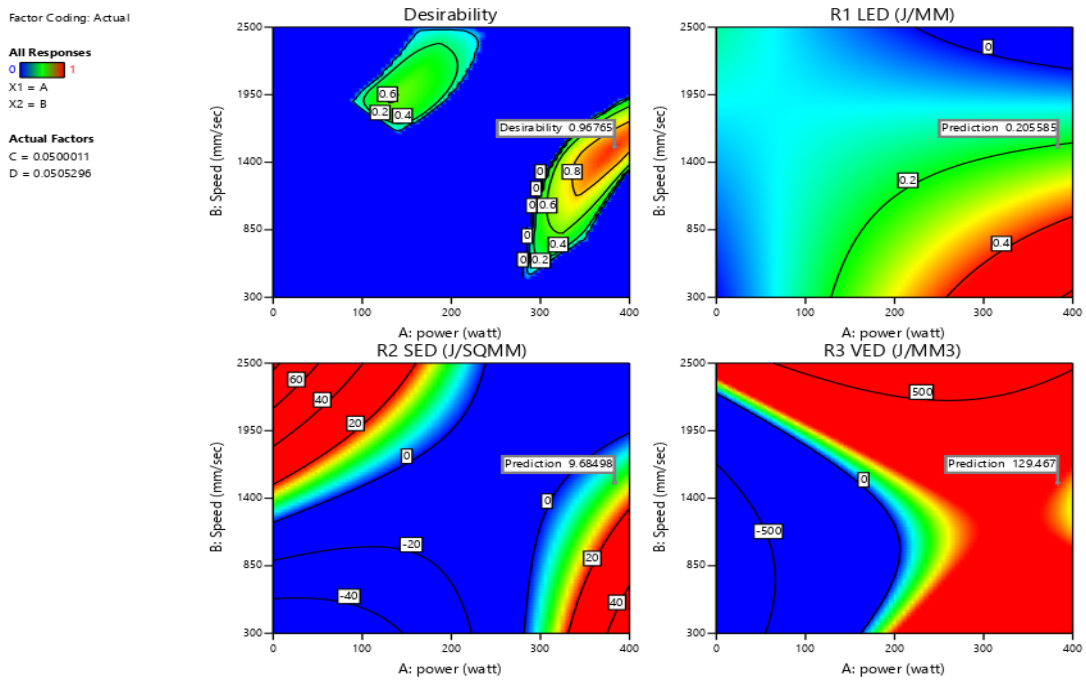

Fig. 5 *Desirability for optimum values of LED, SED, and VED vs speed & power*

4.1.6 Enhancing SLM Performance Through Response Surface Optimization and Efficient Parameter Tuning with Desirability Plots

Precision is crucial when trying to optimize the SLM process. To meet certain criteria, this study concentrated on three key goals: linear energy density, surface energy density, and volume energy density. ANOVA analysis demonstrated the significance of individual parameters by identifying the best combinations of process parameters for each target. Experimental validation of the findings highlighted performance increases. The graph used to evaluate desire showed that 0% desirability is produced by power and speed levels lower than 300 and 850 mm/sec, respectively. On the other hand, when power is 200W and speed is 1400, attractiveness just slightly increases to 0.06.

Desirability varies between 0.2 and 0.8 for powers above 300 and speeds below 1400. with a peak of 96.75, a speed of 1521, a power of 382W, desirability of 96.8%. Notable findings include the power's 300–400 range and speed's 1400–1600 range. In the study, predictions were also made using 3D surface graphs. For power versus speed, the projected value for linear energy density was 0.205 J/mm, whereas the predicted value for surface energy density was 9.86 J/mm^2. The calculated volume energy density of 129.467 J/mm^3 provides important information about the characteristics and behaviors of the materials.

5. Artificial Neural Network

A neural network is a machine that learns by using interconnected neurons or nodes in a layered structure that resembles the human brain it is also defined as an artificial neural network. A neural network can be trained using data. As a result, it can be trained to recognize shapes, classify the data, and predict future events. A neural network's input is divided into layers such as the human brain, which can be trained to recognize patterns in speech or images by exposing it to a variety of examples. Its behavior is determined by how its different components are attached, as well as the weights or strengths, of those interconnections. These weights are impulsively updated throughout training based on a training algorithm till the artificial neural network is completed.

5.1 Levenberg-Marquardt

This approach demands greater recollection but takes significantly less time. When generalization loses its ability to improve, training comes to a standstill. As shown by a deprivation in the mean square error of the validation samples.

	SAMPLES	MSE	R
Training(blue)	25	2.63397e-1	9.98812e-1
Validation (Green)	5	22.49229e-0	9.13338e-1
Testing (Red)	5	18.04831e-0	9.75948e-1

The sum of squared variance between outputs and targets is defined as Mean Squared Error. Smaller values are preferable. Zero means there is no error. The correlation between the targets and outputs is measured by R values. A regression value of 1 denoted a nearer connection, while a regression value of 0 represents a random relationship.

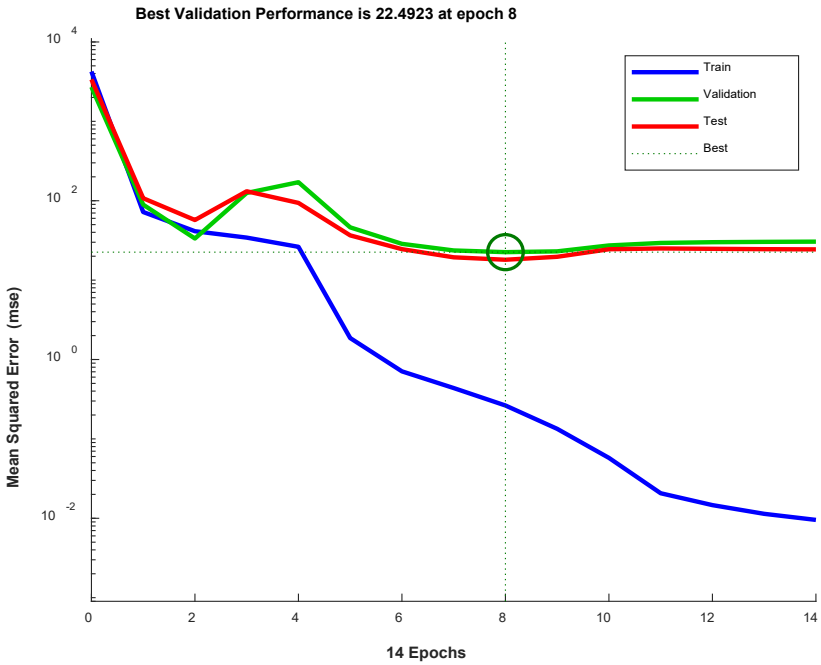

Fig. 7 *Mean squared error with 1000 epochs*

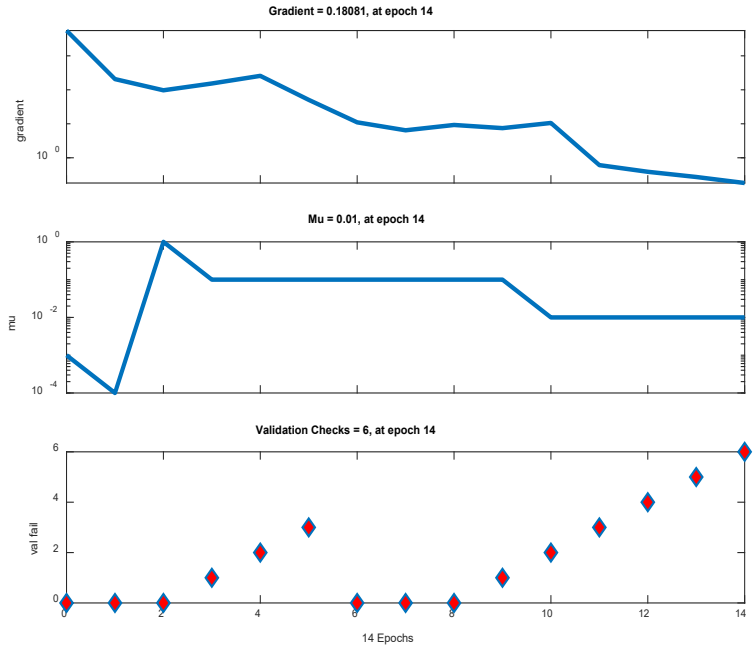

Fig. 8 *Gradient descent*

Int. Journal of Integrated Engineering Vol. 16 No. 3 (2024) p. 358-375

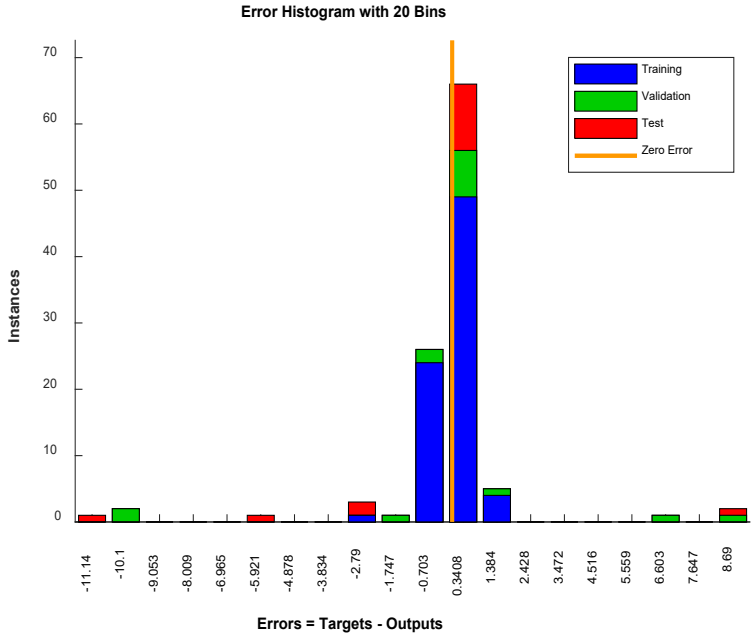

Fig. 9 *Training error using histogram*

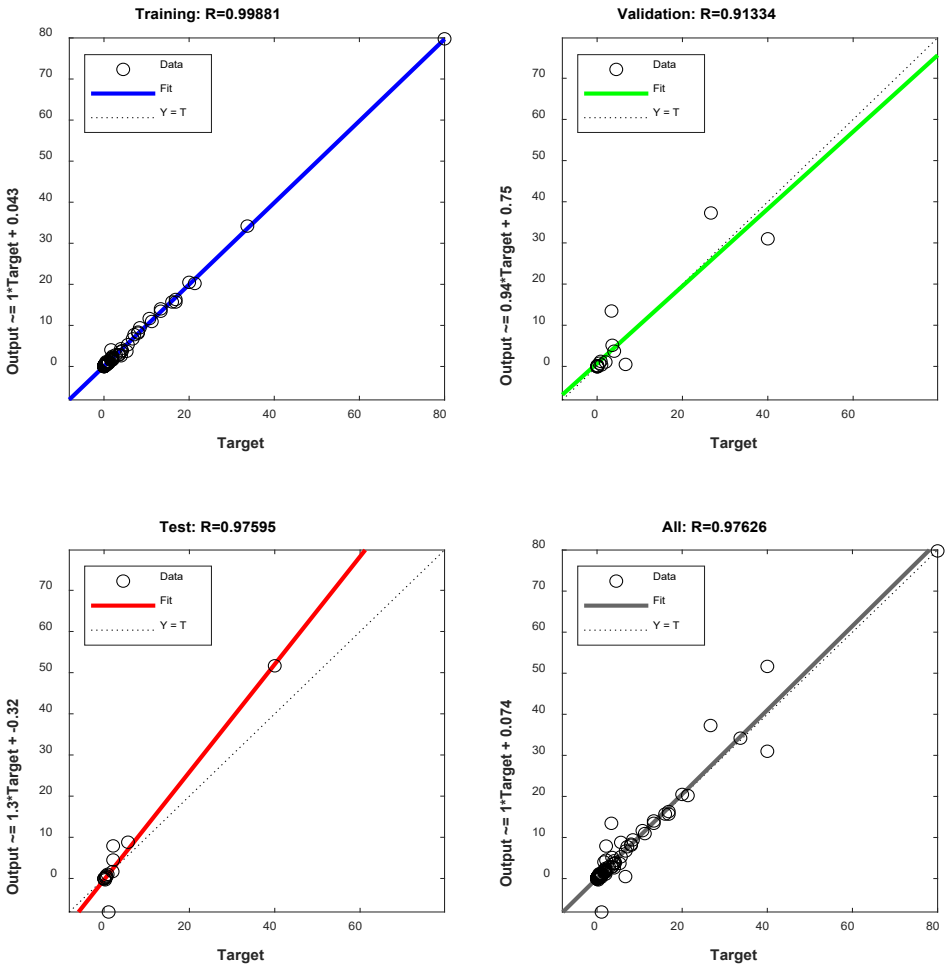

Fig. 10 *Regressions in the training window*

Fig 7 represents the eighth epoch, the MSE (Mean square error) performance is 22.4. Fig 8 depicts gradient descent in the context of the learning training algorithm for the adjustment of neuron weights by evaluating the gradient's loss function. At epoch 14, the gradient value is 18.081 percent, and the correct check is 6. To avoid the training network from performing poorly on non-training, training is halted if validation performance degrades for the default value of 14 epochs. The Error histogram with 20 bins is shown in Fig 9. And is calculated as Error = Target-output. The regression percentage for training is 99 percent, validation is 91 percent, and testing is 97 percent, as shown in Fig 10.

5.2 Bayesian Regularization

This algorithm is typically slower, but it can produce some good generalizations for noisy data, difficult, or small. Training is postponed due to adaptive weight depreciation (regularization).

	SAMPLES	MSE	R
Training(blue)	25	7.52699e-1	9.99999e-1
Validation (Green)	5	0.00000e-0	0.00000e-1
Testing (Red)	5	5.82805e-0	8.24768e-1

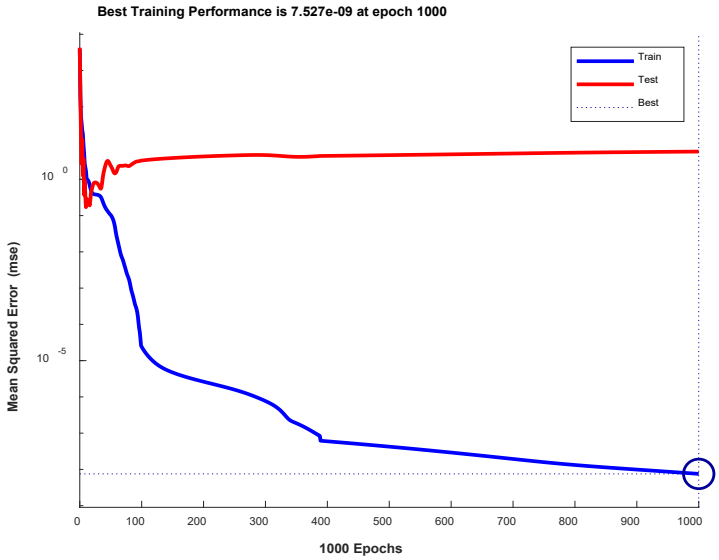

Fig. 11 *Mean squared error with 1000 epochs*

Int. Journal of Integrated Engineering Vol. 16 No. 3 (2024) p. 358-375

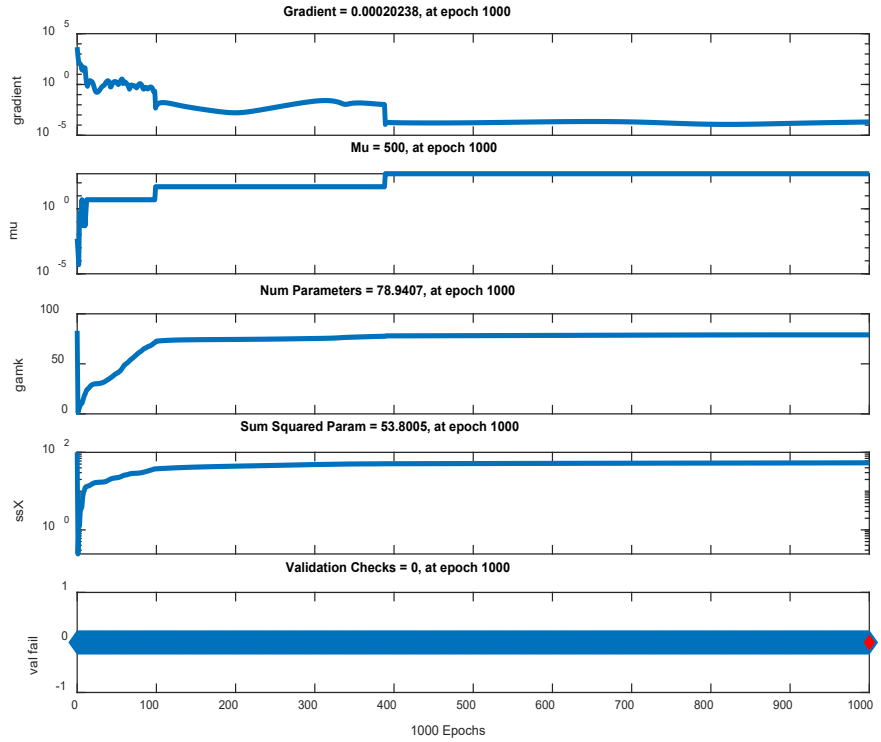

Fig. 12 *Gradient validation*

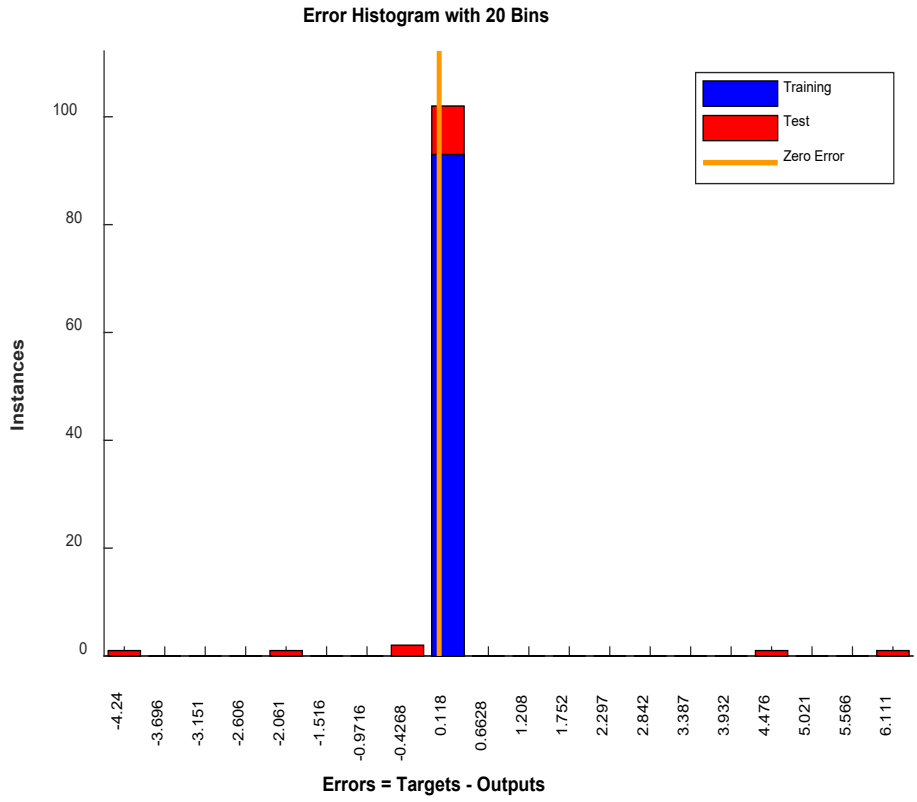

Fig. 13 *Training error using histogram*

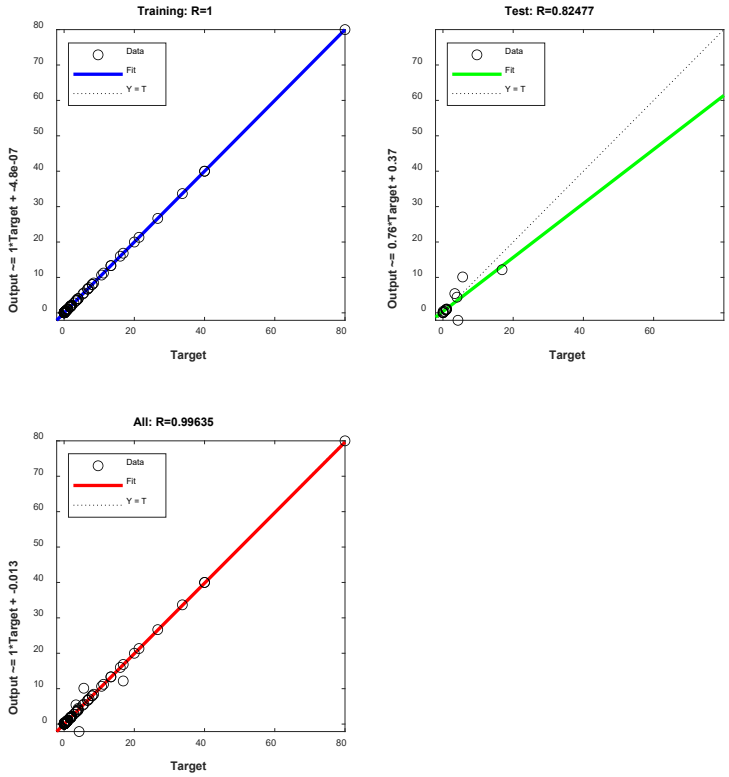

Fig. 14 *Regression in the training window*

Fig. 11 depicts at the 1000 epoch, the MSE (Mean square error) performance is 75%. Fig.12 depicts gradient descent in the context of knowing the backpropagation algorithm for the adjustment of neuron weights by evaluating the gradient's loss function. At epoch1000, the gradient effective parameter value is 78.9 percent, and the number of valid checks is 6. To avoid the training network from performing poorly on non-training, training is delayed if validation performance degrades for the corresponding 1000 epochs. The Error histogram with 20 bins is shown in Fig.13 and is calculated as Error = Target-output. The regression percentage for training is 100%, validation is 82 %, and testing is 97 percent, as shown in Fig 14.

5.3 Scaled Conjugate Gradient

This algorithm necessitates a smaller amount of memory. When generalization decides to stop working to improve, as suggested by an extension in the mean square error of the validation samples, training automatically stops.

	SAMPLES	MSE	R
Training(blue)	25	8.90953e-1	9.96686e-1
Validation (Green)	5	7.88878e-0	9.68914e-1
Testing (Red)	5	4.09369e-1	9.28371e-1

Int. Journal of Integrated Engineering Vol. 16 No. 3 (2024) p. 358-375

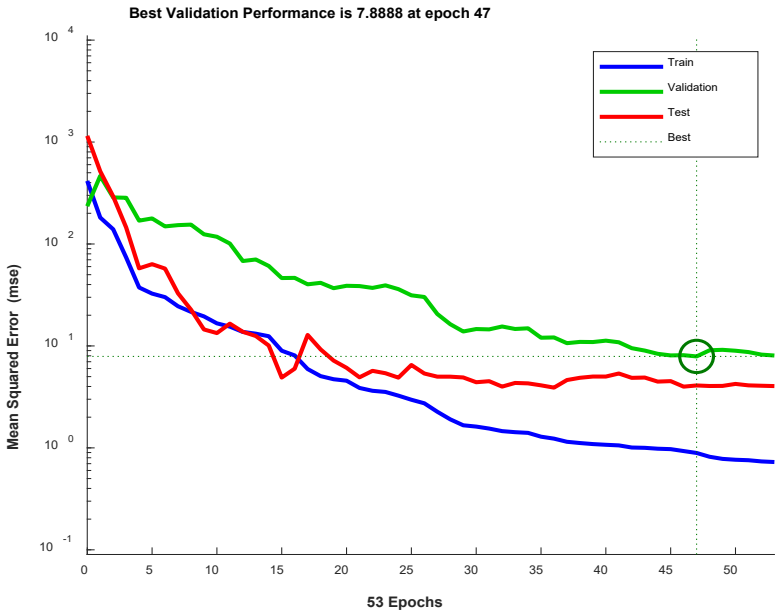

Fig. 15 *Mean squared error*

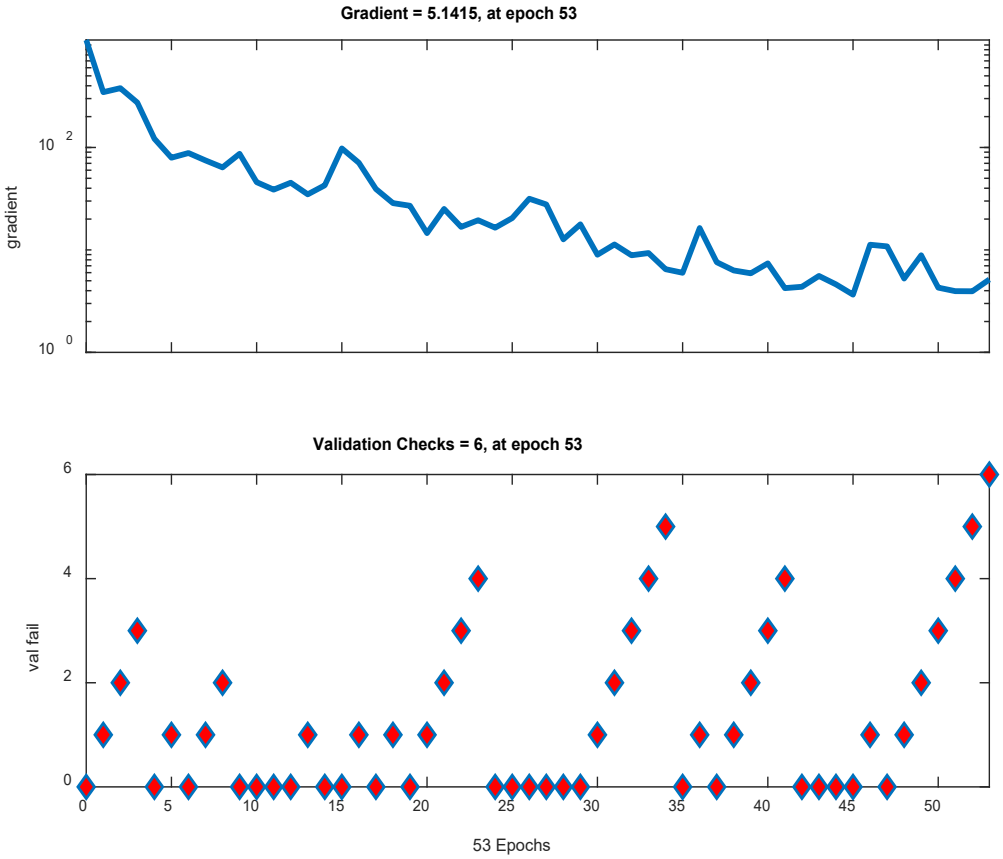

Fig. 16 *Gradient descent*

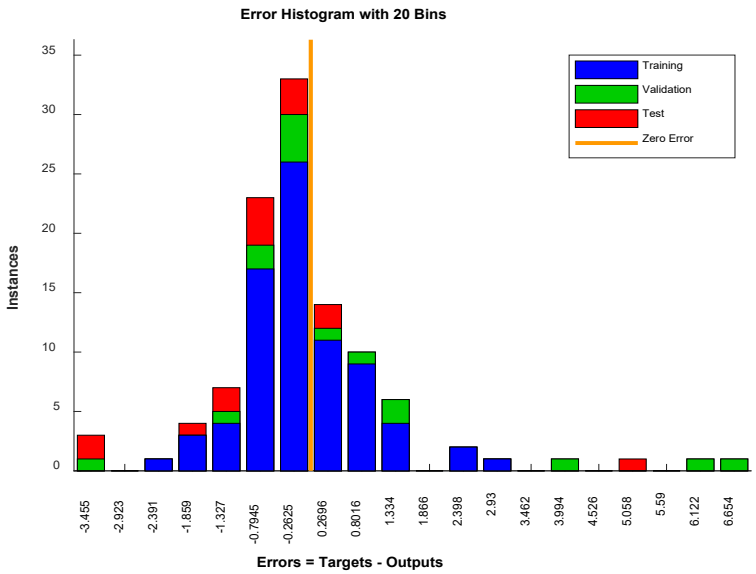

Fig. 17 *Training error histogram with 20 bins*

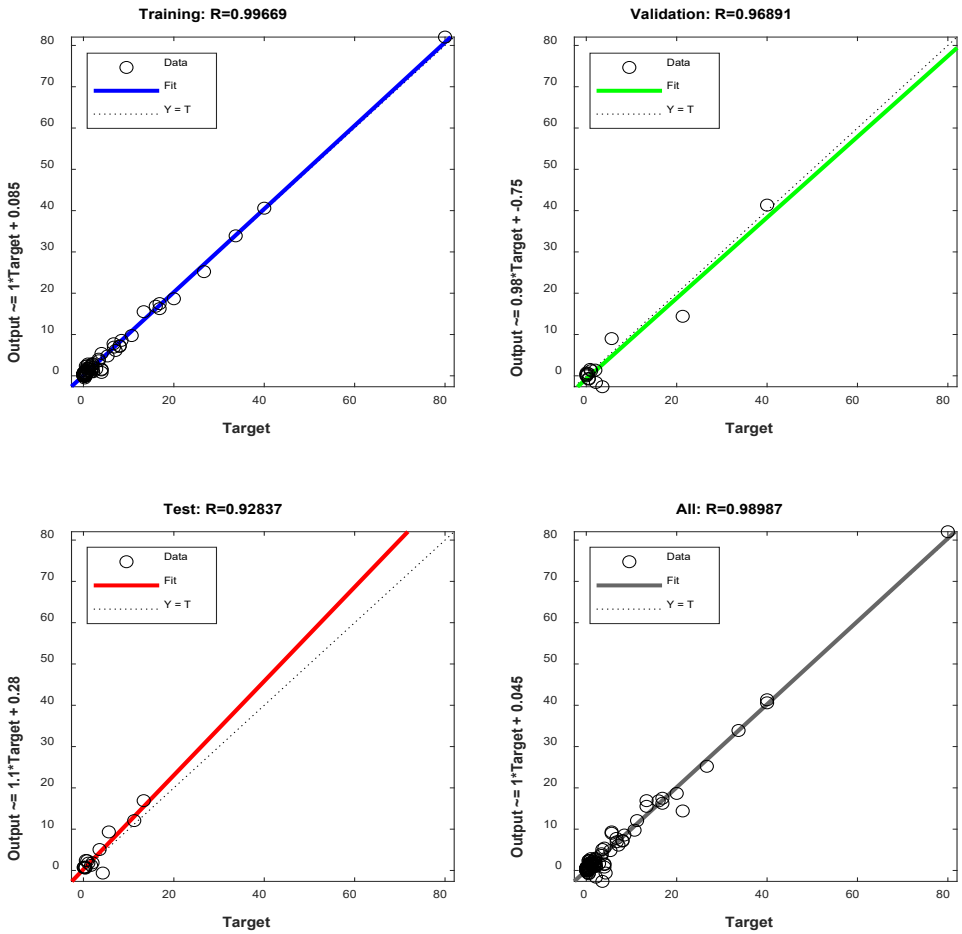

Fig. 18 *Regression in the training window*

Fig. 15 depicts that at the 47epoch, the MSE (Mean square error) performance is 78 percent. Fig 16 depicts the gradient descent in the context of knowing the backpropagation for the adjustment of the weight of the neurons by calculating the loss function of the gradient. At epoch 53, the gradient value is 51.14

percent, and the number of valid checks is 6. To prevent the training network from performing poorly on non-training, training is halted if validation performance degrades for the default value of 14 epochs. The Error histogram with 20 bins is shown in Fig 17 and is calculated as Error = Target-output. The regression percentage for training is 99 percent, validation is 96 percent, and testing is 92 percent, as shown in Fig 18.

6. Conclusion

The ANOVA analysis is critical in determining the best processing variables needed to achieve increased energy density in Selective Laser Melting (SLM) components. These specifications consist of 383.18W power, 1525.4mm/s scanning speed, and 0.050mm hatch spacing. In addition to improving energy density, this parameter combination forecasts LED, SED, and VED values of 0.206 j/mm, 9.685 j/mm^2, and 129.46 j/mm^3 providing a quantitative method for enhancing mechanical performance in SLM and the desirability is 96.8%. The study emphasizes the critical importance of screening designs and the design of experiments (DoE) in revealing the intricate interactions among process variables. These approaches are used in the research to present a systematic approach that reveals complex variables that affect outcomes, improving comprehension and decision-making in a variety of applications, including additive manufacturing. The Artificial Neural Network (ANN) efficiently combines intricate parameters, precisely forecasts results, and streamlines difficult procedures. High R-values and a remarkable R-value of 97%, demonstrating alignment between anticipated and actual results, are evidence of its robustness, according to validation. The research's importance goes beyond SLM to include other manufacturing technologies, improving workflows and product quality through DoE, ANN modeling, and quality prediction.

Acknowledgement

The authors express their gratitude to the technical team at Osmania University, Hyderabad for helping with data collection and experiment setup and to the GPREC Research Centre in Kurnool, Andhra Pradesh, India, for its facilities and support. We also value the advice and perspectives provided by our colleagues.

Conflict of Interest

The authors declare that there is no conflict of interest

Authors Contribution

*The research **framework, trials, and data analysis** were all created by Kalluru Madhurima. Dr. K. Devaki Devi **supervised** the research project, **provided guidance on methodology**, and contributed to the **manuscript preparation and editing**. The final text has been reviewed and approved for submission by both authors.*

References

[1] 3D printing of high-strength aluminum alloys John H. Martin1,2, Brennan D. Yahata1, Jacob M. Hundley1, http://www.nature.com/doifinder/10.1038/nature23894.

[2] Mohsen Mohammadi ∗, Hamed Asgar (2018) Achieving low surface roughness AlSi10Mg 200C parts using direct metal laser sintering. Additive Manufacturing 23-32. https://doi.org/10.1016/j.addma.2017.12.012.

[3] Singamneni S, Yifan LV, Hewitt A, Chalk R, Thomas W, et al. (2019) Additive Manufacturing for the Aircraft Industry: A Review. J Aeronaut Aerospace Eng 8: 214. doi:10.4172/2329-6542.1000214.

[4] W. Yu, S.L. Sing, C.K. Chua, X. Tian, Influence of re-melting on surface roughness and porosity of AlSi10Mg parts fabricated by selective laser melting, Journal of Alloys and Compounds (2019), DOI: https://doi.org/10.1016/j.jallcom.2019.04.017. Acta Materialia, Volume 61, Issue 5

[5] Umberto Scipioni Bertoli a, Alexander J. Wolfer b, On the limitations of Volumetric Energy Density as a design parameter for Selective Laser Melting, Materials & Design Volume 113, 5 January 2017.

[6] HuZhang, HaihongZhu, TingQiZhihengHu, XiaoyanZeng, Selective laser melting of high strength Al–Cu–Mg alloys: Processing, microstructure and mechanical properties, Materials Science and Engineering: Volume 656, 22 February 2016, https://doi.org/10.1016/j.msea.2015.12.101.

[7] Wei Pei, Wei Zhengying, Chen Zhen, Du Jun, He Yuyang, Li Junfeng, Zhou Yatong, The AlSi10Mg samples produced by selective laser melting: single track, densification, microstructure, and mechanical behavior, http://dx.doi.org/doi:10.1016/j.apsusc.2017.02.215.

[8] Minghuang Zhao, Changhong Duan, and Xiangpeng Luo, Metallurgical defect behavior, microstructure evolution, and underlying thermal mechanisms of metallic parts fabricated by selective laser melting additive manufacturing, Published under license by Laser Institute of America. https://doi.org/10.2351/1.5141074.

[9] A. Ramya and Sai Leela Vanapalli, 3d Printing Technologies in Various Applications. International Journal of Mechanical Engineering and Technology, 7(3), 2016, pp. 396–409.
[10] John J. Lewandowski and Mohsen Seif, Metal Additive Manufacturing: A Review of Mechanical Properties, DOI: 10.1146/annual-mat sci-070115-032024.
[11] Analysis and Optimization of Machining Process Parameters Using Design of Experiments Dr. M. Naga Phani Sastry, K. Devaki Devi, Dr, K. Madhava Reddy, Industrial Engineering Letters www.iiste.org ISSN 2224-6096 (Paper) ISSN 2225-0581 (online) Vol 2, No.9, 2012.
[12] Enzo Grossi and Massimo Buscemab, Introduction to artificial neural networks, Article in European Journal of Gastroenterology & Hepatology · January 2008 DOI: 10.1097/MEG.0b013e3282f198a0.
[13] Nelson J. C., Xue S., Barlow J. W, Beaman J J, Marcus H L, and Bourell D L 2002 Model of the selective laser sintering of bisphenol-A polycarbonate Ind. Eng. Chem. Res. 32 2305–17
[14] Yardimci M A, Guceri S I and Danforth S C 1995 A phenomenological numerical model for fused deposition processing of particle-filled parts 1995 Int. Solid Freeform Fabrication Symp. (https://doi.org/10.15781/T2NV99W2B)
[15] Trevisan F, Calignano F, Lorusso M, Pakkanen J, Aversa A, Ambrosio E, Lombardi M, Fino P and Manfredi D 2017 On the selective laser melting (SLM) of the AlSi10Mg alloy: process, microstructure, and mechanical properties Materials 10 76
[16] Francesco Trevisan 1,2, Flaviana Calignano 2, Massimo Lorusso 2, Jukka Pakkanen 1,2, Alberta Aversa 1, Elisa Paola Ambrosio 2, Mariangela Lombardi 1, Paolo Fino 1,2 and Diego Manfredi 2,* On the Selective Laser Melting (SLM) of the AlSi10Mg Alloy: Process, Microstructure, and Mechanical Properties, Materials 2017, 10, 76; doi:10.3390/ma10010076.
[17] Gupta A K, Lloyd D J and Court S A 2001 Precipitation hardening in Al-Mg-Si alloys with and without excess Si Mater. Sci. Eng. A 316 1–2
[18] SEVIMEC, EL PROCESO DE MECANIZADO. [https://sevimec.es/es/el-proceso-demecanizado, January 12, 2017] Kumar S 2014 Selective laser sintering/melting Comprehensive Mater. Process. 10 93–134
[19] Qiu C, Panwisawas C, Ward M, Basoalto H C, Brooks J W and Attallah M M 2015 On the role of melt flow into the surface structure and porosity development during selective laser melting Acta Mater. 96 72–79
[20] [21] Kruth J P, Froyen L, van Vaerenbergh J, Mercelis P, Rombouts M and Lauwers B 2004 Selective laser melting of iron-based powder J. Mater. Process. Technol. 149 1–3
[21] Qiu C, Adkins N J E and Attallah M M 2013 Microstructure and tensile properties of selectively laser-melted and of HIPed laser
[22] Jensen, W.A.: Response surface methodology: process and product optimization using designed experiments. J. Qual. Technol. 49(2), 186 (2017)
[23] Montgomery, D.C.: Design and Analysis of Experiments, Student Solutions Manual, p. 248. Wiley, New Jersey (2012)
[24] Paulo Davim, J.: Design of Experiments in Production Engineering. Management and Industrial Engineering, p. 196. Springer International Publishing Switzerland, Aveiro, Portugal (2016)
[25] Chowdhury, S., & Anand, S. (2016). Artificial Neural Network Based Geometric Compensation for Thermal Deformation in Additive Manufacturing Processes. Volume 3: Joint MSEC-NAMRC Symposia. doi:10.1115/msec2016-8784
[26] [Sondagar, H., Bhadauria, S. S., & Sharma, V. S. (2021). Artificial neural network (ANN) based prediction of process parameters in additive manufacturing. IOP Conference Series: Materials Science and Engineering, 1136(1), 012026. doi:10.1088/1757-899x/1136/1/012026 Akbari M et al 2016 J. Optik 127 11161–172.
[27] Wang, G., Huang, L., Liu, Z., Qin, Z., He, W., Liu, F., … Nie, Y. (2020). Process optimization and mechanical properties of oxide dispersion strengthened nickel-based superalloy by selective laser melting. Materials & Design, 188, 108418. doi: 10.1016/j.matdes.2019.108418
[28] Jensen, W.A.: Response surface methodology: process and product optimization using designed experiments. J. Qual. Technol. 49(2), 186 (2017)
[29] Paulo Davim, J.: Design of Experiments in Production Engineering. Management and Industrial Engineering, p. 196. Springer International Publishing Switzerland, Aveiro, Portugal (2016)